Applying refraction traveltime migration to image bedrock with high resolution

Yihao Wang, Jie Zhang, University of Science and Technology of China (USTC)*

Summary

In the near-surface velocity structure estimation, first-arrival traveltime tomography tends to produce a smooth velocity model. If the true shallow structures include a weathering layer over a high-velocity bedrock, the first-arrival traveltime tomography may fail to produce the sharp interface. In that situation, refraction traveltime migration proves to be an effective tool for mapping the refractor with high resolution. The method involves the reconstruction of the forward and backward wavefront in the subsurface by applying a wavefront raytracing method. Subsequently we apply Hagedoorn imaging condition to generate the precise shape of the high-velocity refractor. We analyze the uncertainty of refraction traveltime migration with synthetic tests. For a real dataset, we first apply first-arrival traveltime tomography to produce a velocity model, and then apply refraction traveltime migration to image the refractor. Constructing a velocity model with inclusion of the refractor, we are able to compute long-wavelength statics corrections helping to improve CMP stacking quality.

Introduction

Refraction traveltime migration method is mainly based on two important steps: wavefront reconstruction and applying imaging condition. The wavefront reconstruction method is one of the earliest methods to interpret refraction traveltimes. Thornburgh (1930) presents an approach to reconstruct wavefront by applying the Huygen's principle in reverse time. Hagedoorn (1959) improves the method and demonstrates an imaging condition to locate the refracting horizon. Those two methods employ a manual graphical mapping method. Aldridge and Oldenburg (1992) first utilize the finite-difference traveltime method to reconstruct wavefront on computer. Zhang and Toksöz (1997) apply an improved minimum-traveltime method for the traveltime downward continuation and develop the concept of refraction traveltime migration.

In this study, we apply refraction traveltime migration method developed by Zhang and Toksöz (1997) to image synthetic and real data. We shall analyze the influence of different factors on the final migration results and find out when this method is acceptable and stable. The method is also tested with a complex land dataset with moderate lateral velocity variations, and the resulted refractor is applied as the intermediate datum in statics calculation, to improve the lateral continuity of CMP reflection stack.

Wavefront Reconstruction

Following Thornburgh (1930), we reconstruct two wavefront systems that propagate oppositely. We select the forward and reverse spread arrival times, respectively. Then we apply the improved minimum-traveltime method to calculate the subsurface wavefront (Zhang and Toksöz, 1997).

The downward continuation of two wavefront systems are completed by activating a line source at the receiver array each time, respectively. The line source is activated sequentially with an initiation equation $T_s(X)$:

$$T_s(X) = T_r - T(X) \qquad (1)$$

where T_r is the reciprocal time and $T(X)$ is the recorded arrival time.

According to the characteristics of the first arrivals, there is a blind area for refraction at the near offset. In order to better image the edge of the refractor, we replace the near-offset traveltimes of a shot with the corresponding offset shots to construct phantomed arrivals, as shown in Figure 1 (Ackermann et al., 1986).

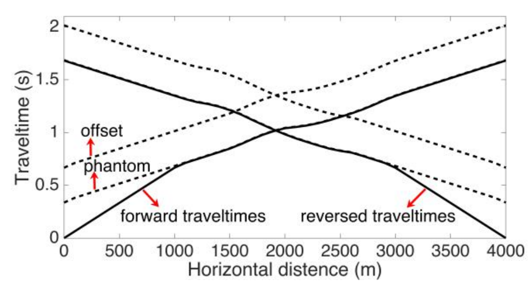

Figure 1: Forward, reverse, and offset traveltimes for a two-layer model with a constant overburden velocity. The near-offset forward and reverse traveltimes are phantomed by the offset shots.

Imaging Condition

Hagedoorn (1959) elucidates an imaging condition to locate the refracting horizon. For each subsurface point, when the summation of the forward propagating wavefront system with the traveltime t_f and the reverse propagating wavefront system with the traveltime t_r equals to the reciprocal time T_r, the point should be just on or slightly below the refracting interface:

$$t_f(x,z) + t_r(x,z) = Tr \quad (2)$$

The grid points which satisfy the imaging condition represent the position of the refractor. If the condition cannot be satisfied right on a grid point but between two grid points, we simply apply linear interpolation to determine the actual position of the refractor.

Synthetic Tests

To evaluate the performance of the migration method, we design several synthetic tests with 2D velocity models. First, we test the feasibility of this method with a simple two-layer velocity model. Then, considering the real situation, there are several factors that may affect the performance, including the reciprocal time, the accuracy of overburden velocity, and the picked first-arrival traveltime. Therefore, we further design several tests to validate the method.

Figure 3a displays the true model of the following four synthetic tests. The horizontal length of the model is 4000 m, and the depth range is 500 m. There are 2 shots with 4000 m apart and 41 receivers with 10 m spacing, as shown in Figure 3a by red and yellow dots, respectively. There are both a depressed and an elevated subsurface structures in Figure 3a with a 1500 m/s overburden velocity and 3000 m/s velocity beneath the refractor.

(a)

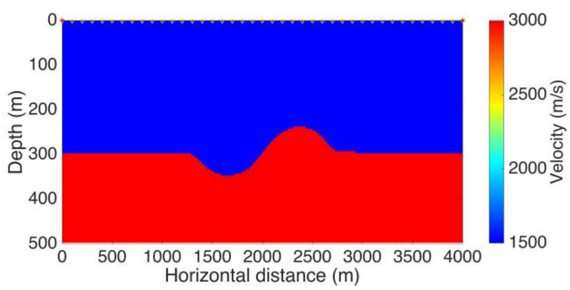

(b)

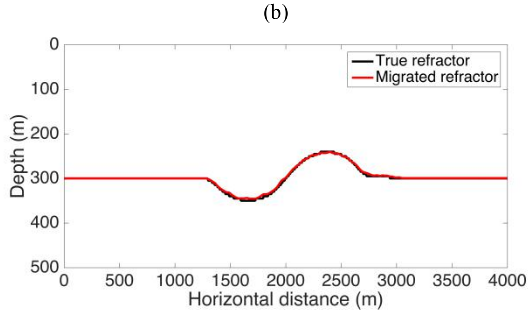

Figure 3: (a) The true model of the synthetic test. (b) The result of refraction traveltime migration method versus the true position of the refractor.

We first test a simple two-layer velocity model to verify the reliability of the method. We pick the first-arrival traveltimes of both the forward and reverse shots, respectively. Then we only need to acquire the overburden velocity for the need of migration by utilizing the direct wave arrivals. In real cases, the velocity model is usually obtained by applying first-arrival traveltime tomography method, which will be discussed in the last test. Further, we apply the wavefront reconstruction approach and the imaging condition to image the refractor. The result is displayed in Figure 3b, matching the true refractor very well.

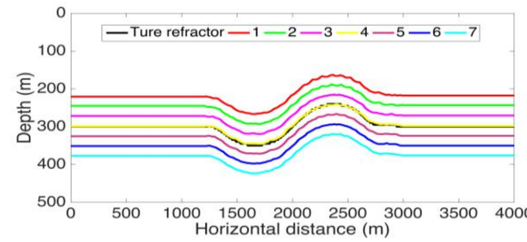

Figure 4: Results of refraction traveltime migration method with different reciprocal times. The differences between the true and the input reciprocal time are -90 ms, -60 ms, -30 ms, 0 ms, 30 ms, 60 ms, and 90 ms.

Reciprocal time is employed in calculating the new line source and applying the imaging condition, thus, we should discuss the impact of the parameter. In real cases, a receiver cannot be placed right at the position of a source, therefore, the reciprocal time is calculated through interpolation. The picked first-arrival traveltimes may also include errors, leading to errors in reciprocal times. Figure 4 shows the test with uncertainties in reciprocal times, varying from -90 ms to 90 ms. We can see the depth of refractor changing with different reciprocal times. When the reciprocal time is too long or too short, the depth of the refractor is imaged too deep or too shallow, respectively. But the shape of the refractor remains unchanged. This observation is important, because it tells that error in reciprocal time should not affect the shape of refractor, which is important for statics corrections.

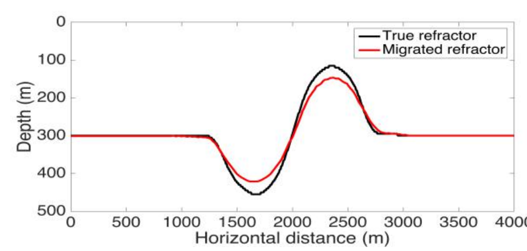

Figure 5: The result of refraction traveltime migration method compared to the position of the true refractor.

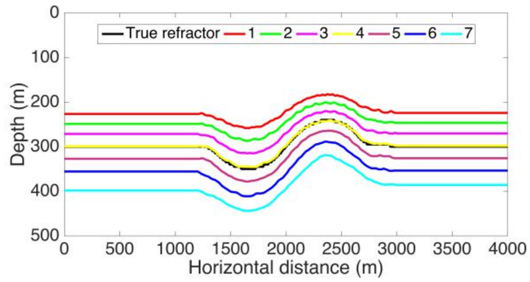

Figure 6: The result of refraction traveltime migration method with different velocity models. The differences between the true and the input migrated velocity of model 1 to 7 are -300 m/s, -200 m/s, -100 m/s, 0 m/s, 100 m/s, 200 m/s, and 300 m/s.

(a)

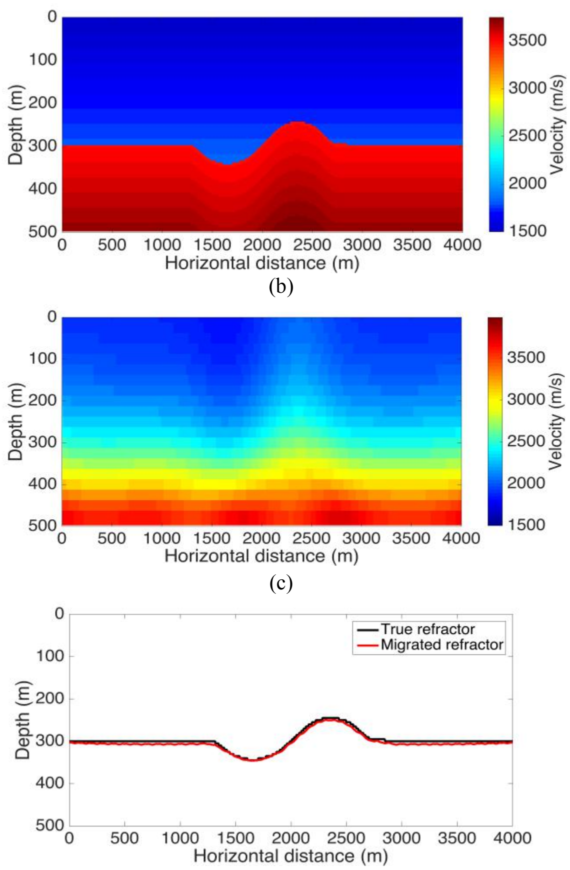

Figure 7: (a) The true model. (b) The migration model from the first-arrival traveltime tomography method. (c) The result of refraction traveltime migration method compared to the position of the true refractor.

Then, we analyze the impact of uncertainty in picked traveltimes on the refractor imaging. The Hagedoorn imaging condition requires traveltimes of refraction waves. However, because of the complex subsurface structure, the head wave we pick might be diffractions, diving waves, or reflections. As shown in Figure 5, if the undulating interface of a refractor varies too much, the first-arrivals may not propagate along the interface, the refractor image could be close to the actual shape but losing its accuracy.

Similar to reflection migration, the velocity input is an important part in refraction traveltime migration. Figure 6 displays the refraction imaging results with different input velocity for migration, with the velocity error varying from -300 m/s to 300 m/s. As we can see, the depth of the refractor becomes deeper with a faster velocity, but the refractor shape is well maintained.

The overburden velocity can be varied in real cases, thus, we test refraction traveltime migration in that situation. Figure 7a shows a synthetic true model with a vertical velocity gradient in the top layer. We first apply the first-arrival traveltime tomography method to invert the velocity model. The inverted result is displayed in Figure 7b. Figure 7c shows the comparison between the refraction traveltime migration image using the tomographic velocity and the true refractor. The results are nearly identical to the true interface.

Real Data Application

We apply the above method to real data. This dataset includes 476 shots with the shot interval of about 10 m, and 1735 receivers with the receiver interval of about 10 m. For every shot, there are about 480 receivers.

In real situation, the receivers of a shot cannot cover the entire surface area but only certain offset. Therefore, we first shift and merge refraction traveltimes of each shot to create two new traveltime curves virtually from the very left shot and the very right shot. We also need to calculate the phantomed arrival times to replace the direct waves within 800 m offset. Then, we derive a smooth velocity model by applying the first-arrival traveltime tomography method, as shown in Figure 8a. The average reciprocal error of the picks is approximately 4 ms, and the misfit is 3.976 ms. Finally, we utilize the velocity model from the first-arrival traveltime tomography as the migration velocity to perform refraction imaging. The black line in Figure 8b shows the migrated refractor.

In order to verify the reliability of the result, we compare the performance of it with a line chosen from the migrated velocity model, which is the black line shown in Figure 8a, as the intermediate datum to calculate the long-wavelength shots and receivers statics. The red line in Figure 8a and Figure 8b represent the same floating datum which is determined according to the geometry.

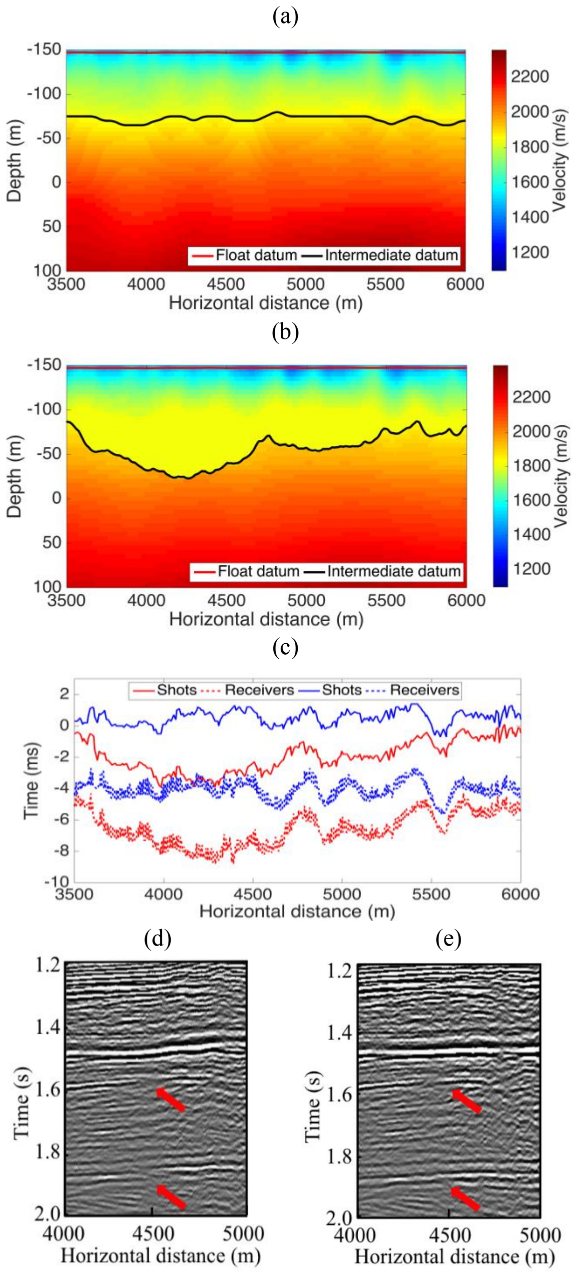

Figure 8: (a) The velocity model from the first-arrival traveltime tomography method. Red line denotes the floating datum. Black line denotes the intermediate datum. (b) The constructed velocity model with migrated refractor. Red line denotes the floating datum. Black line denotes the migrated refractor. (c) The long-wavelength statics based on different models and intermediate datum. Red lines represent the one with migration results, blue lines show the results using standard tomography. (d) The CMP stacking results using statics from model (a). (e) The CMP stacking results using statics from model (b).

Considering the true subsurface structure, where exists sharp interfaces with clear velocity contrast, we improve the velocity model by applying downward continuation method to the overburden velocity from the position slightly above the refractor, as shown in Figure 8b. Figure 8c depicts the comparison of the statics. Between the distance of 4000 m and 5000 m, we can see obvious differences in both shot statics and receiver statics. Figure 8d and Figure 8e show the CMP stacking results, utilizing the information of Figure 8a and Figure 8b as input, respectively. As we can see from red arrows, the image applying the result of refraction traveltime migration shows improvement in lateral continuity of reflectors. It suggests that refraction traveltime migration improves the accuracy of statics correction by producing a precise refractor and an accurate velocity model.

Conclusions

Refraction traveltime migration is a unique approach for mapping near-surface refractor with high resolution. Our numerical analysis suggests that the shape of refraction traveltime migration image is insensitive to reciprocal time, migration velocity, and structure variations. Therefore, it is a good approach if it combines with first-arrival traveltime tomography first for resolving the migration velocity. It helps solve a problem in the traveltime tomography, which tends to produce smooth refractor image.

Acknowledgments

We appreciate the support of GeoTomo, for allowing us to utilize the software package and perform this research. We thank the National Science Foundation of China (Grant No. No. 41674120).